Hindawi
Geofluids
Volume 2022, Article ID 2700084, 14 pages
https://doi.org/10.1155/2022/2700084

Research Article

Study on the Coevolution Mechanism of Slope and Prevention Structures under Rainfall

Lin Tang[1], **Daoyong Wu**[1], **Honggang Wu**[1,2], **Hong Wei**[1], **Jun Pang**[3], **Wei Guan**[1] and **Hao Sun**[4]

[1]*College of Resources and Environmental Engineering, Key Laboratory of Karst Georesources and Environment, Ministry of Education, Guizhou University, Guiyang, 550025 Guizhou, China*
[2]*China Northwest Research Institute Co. Ltd. of CREC, Lanzhou, 730070 Gansu, China*
[3]*College of Civil Engineering, Lanzhou Jiaotong University, Lanzhou, 730070 Gansu, China*
[4]*College of Civil Engineering and Architecture, Southwest University of Science and Technology, Mianyang 621000, China*

Correspondence should be addressed to Daoyong Wu; wdy123456@yeah.net

Received 11 February 2022; Accepted 11 April 2022; Published 4 May 2022

Academic Editor: Dongdong Ma

Copyright © 2022 Lin Tang et al. This is an open access article distributed under the Creative Commons Attribution License, which permits unrestricted use, distribution, and reproduction in any medium, provided the original work is properly cited.

The relationship between slope and prevention structures under the action of rainfall is complicated. In this paper, a series of model tests were carried out to study the coevolution mechanism of slope and prevention structures under rainfall. It was found that the prestressed grouting steel anchor tube frame beam composite structure has a good reinforcement and protective effect on the slope. Specifically, less damage degree is observed for a slope with prestressed grouting steel anchor tube frame beam, while the slope of without prestressed grouting steel anchor tube frame beam suffers from severe deformation. Under the effect of rainfall, the evolution process of slope and prevention structure cooperative deformation can be divided into three stages: creep stage, extrusion stage, and acceleration stage. The antisliding force provided by the prevention structure is positively correlated with the slope deformation. Moreover, as an initiating factor for changes in various monitoring parameters, rainfall plays a dominant role in the variation of earth pressure reinforcement by steel anchor tube.

1. Introduction

Rainfall is one of the most important factors that induce landslides, and there are countless landslides caused by rainfall all over the world [1, 2]. About 90% of landslide disasters in China alone are directly or indirectly related to rainfall by records [3–6]. The occurrence of landslides seriously endangers the safety of human life and property and causes the loss of national economic property [7]. Therefore, the protection and treatment of landslides have always been a concern of people. Advanced and effective treatment measures can effectively treat landslides and avoid disasters caused by landslides, which is the goal of continuous research and exploration. A large number of scholars have studied the reinforcement mechanism of different reinforcement methods and the coevolution mechanism of different prevention structures and slopes by using numerical simulation and model tests [8–11]. However, the synergistic relationship between the slope and the prevention structure is very complicated, and the infiltration of rainfall into the soil further aggravates this complicated relationship. Understanding the synergistic relationship between the slope and the prevention structure is conducive to further improving and perfecting the reinforcement technology. Therefore, an experimental study on the mechanism of synergistic evolution of slopes and protective structures under the action of rainfall was carried out. This research adopts a new type of prevention structure, namely, prestressed grouting steel anchor tube frame beam, and studied the coevolution mechanism between it and the slope by model tests. Additionally, setting up a control test to verify its reinforcement performance.

The prestressed grouting steel anchor tube is an improved structure based on prestressed anchor cable, and

the prestressed anchor cables are usually used with antislide piles. The formation of antislide piles with prestressed anchor cables mainly starts with antislide piles, besides, as an excellent measure for slope reinforcement, antislide piles are widely used in slope reinforcement projects [4–6]. The synergy between antislide piles and slopes has been studied at home and abroad [10, 12–16]. For example, Chen et al. [17] studied the failure mechanism of antisliding piles on a road cutting slope and believed that the direct removal of the slope in front of the pile without using anchor cables was the direct cause of the damage of antisliding piles. Moreover, continuous rainfall over several days aggravated the landslide damage because of the increase of the self-weight and degradation of the mechanical parameters of the slope materials. As a result, the damage of the antislide piles is aggravated. However, the local reinforcement of the slope and the protection of the slope surface by antislide piles are big defects. Therefore, researchers continue to improve on the basis of the antislide pile reinforcement method and gradually form a prestressed anchor cable antislide pile frame beam slope reinforcement structure, which gets a lot of attention and researches [18–20]. Wu et al. [21] and Fan et al. [22] studied the dynamic response of slope reinforced by prestressed anchor cable and antislide pile by indoor shaking table test. Fan et al. [23], Branco et al. [24], and Bathurst et al. [25] studied the control effect of anchor cable antislide pile reinforcement on slope sliding, showing that the protective structure has good reinforcement and protection performance on slopes and slope surfaces. In addition, some scholars have studied the reinforcement characteristics of anchor cables in the roadway, surrounding rock, carrying out optimization research on the reinforcement parameters in these projects [4–6, 26].

In recent years, with the development of slope protection technology towards lighter weight and durability, the previous protection technology cannot meet the durability requirements. Therefore, the grouting steel anchor tube reinforcement technology emerged at the times required, becoming a new research boom in slope reinforcement technology in recent years. Wang et al. [27, 28] have studied the horizontal bearing capacity of vertical steel anchor tube micropile through a large-scale model groove test. Chen et al. [29] carried out a full-scale model test on the antisliding characteristics of the high-pressure grouted steel anchor tube micropile and discussed the antisliding characteristics of the high-pressure grouted steel anchor tube micropile under real stress conditions. Zhang et al. [30] used on-site large-scale model tests to study the new protection technology of grouting steel anchor tube pile group structure and its mechanism. Zhou et al. [31] used on-site prototype tests to study the antisliding performance of the grouted steel anchor tube single pile from the aspects of landslide thrust, pile side earth pressure, pile body bending moment, etc., analyzing the failure of the grouted steel anchor tube.

In conclusion, the grouting steel anchor tube reinforcement technology has gradually become a hot issue, while most of the current research is mainly limited to the active reinforcement performance of the grouted steel anchor tube structure itself. The research on the synergy between slope and protective structure is especially scarce. This article relies on the entity engineering of the diseased slope treatment of DaYangyun Expressway, combining the prestressed grouting steel anchor tube with the frame beam structure and carrying out the model test study of the coevolution of the slope and the prestressed steel anchor tube frame beam under the action of rainfall. The experiment results compared the deformation and failure of the side slope without the prestressed steel anchor tube frame beam to verify the reinforcement performance of the prestressed steel anchor tube frame beam. It is expected to provide a reference for follow-up theoretical research and engineering application and the research on the coevolution mechanism between the new technology of the prestressed grouting steel anchor tube and the slope.

2. Analysis of Engineering Geological Characteristics

The study is based on the diseased slope of section K77 + 775 of DaYangyun Expressway, located in XiShan Township, ErYuan County, Yunnan Province. It belongs to the middle-low mountain geomorphological region of tectonic erosion, altitude between 2240~2290 m with sparse vegetation on the slope. Overall, the slope is relatively flat, between 15°~30°, the slope aspect is SW5°, and the route direction is NW84°. There is no fault structure in this area, the schistosity development of rock mass, and the dominant occurrence of strata is 123°∠ 32°. The slope, a red-bedded geological body, overlies gravel soil of 2-10 m and underlies highly weathered argillaceous siltstone and highly weathered silty mudstone, and the joint fissure has developed. Therefore, the engineering geological characteristics of rock mass itself are relatively weekly. Due to the site investigation time as rainy season, the foot of the slope accumulated water, and the surface drainage was slow, causing part of the surface water to seep through the surface overburden to the foundation interface, which softens the rock mass. The factors provide favorable conditions for the development of slope damage.

An overview of the diseased slope area is shown in Figure 1. The proposed road passes through the foot of the slope in the form of excavation, resulting in the free face being formed at the front edge of the slope. Because of the strong construction disturbance, the original stress balance of the soil is destroyed. Under the interaction of groundwater, rainfall, and other factors, it is easy to form shear cracks at the excavation site of slope construction. According to the field investigation, there are some collapses at the front edge of the slope shown as cracks at the rear edge and dislocation steps and appeared obvious shear cracks on the firstly-level slope. Combined with the phenomenon of drilling core exposure: during core drilling, which was very fast at 18.5 ~ 20 m, the core is disordered and accompanied by signs of rubbing, which presumably a sliding belt, it is the representation of slope deformation sliding.

Based on the above analysis, the slope is currently in an unstable state, it is speculated that further engineering disturbance, heavy rainfall, or continuous rainfall will induce

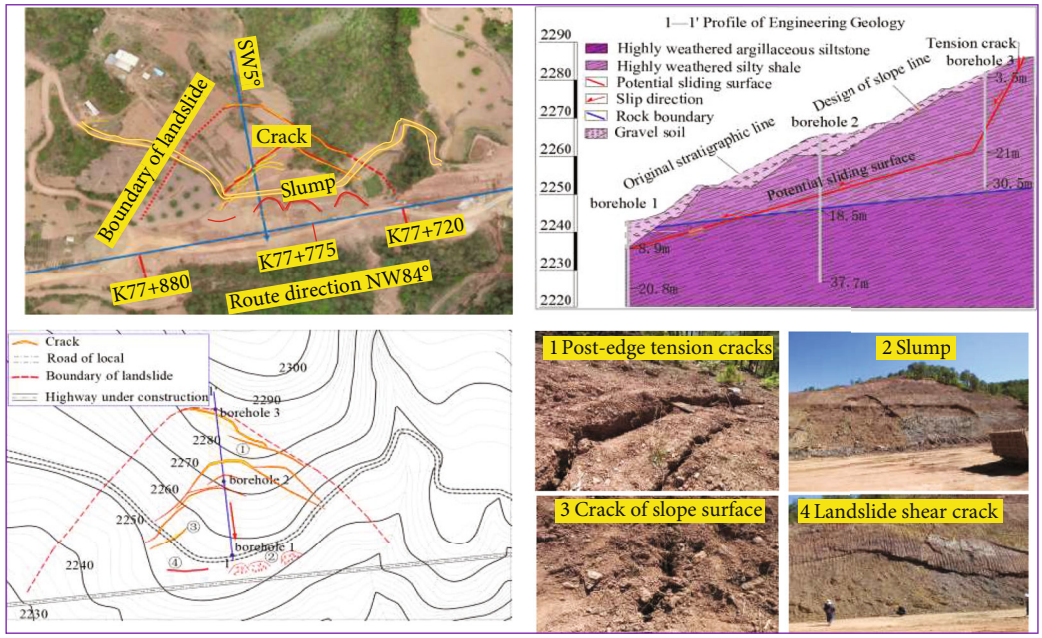

Figure 1: Overview of the landslide area.

landslides. The length of the diseased slope is about 97.5 m, the width is about 160 m, the sliding depth is about 20 m, and the volume of the landslide is $3.12 \times 105\ m^3$, which belongs to a large middle-level landslide, the main sliding direction is 185°.

3. Reinforcement Mechanism of Prestressed Grouting Steel Anchor Tube Frame Beam Composite Structure

Prestressed grouting steel anchor frame beam composite structure is a new reinforcement technology that combined "splitting grouting" and "prestressed anchorage." The steel anchor tube is not only used as a protective measure but also as a channel for grouting, and the rock and soil around the drilling are compacted by splitting grouting, forming a grouting inclusion of "tree root" [30, 32]. Increasing the bonding strength between the grouting body and the rock mass and improving the anchoring force between the grouting body and the rock mass, the steel anchor tube was integrated with the surrounding soil, improving the strength of the surrounding soil. By implanting steel strands inside the steel anchor tube and applying to prestress to the steel strands, the bond strength between splitting grouting and rock mass was fully exerted, and the anchoring force is further improved. At the same time, it can also increase the shear strength of the anchor cable and improve the strength parameters of the sliding zone rock mass. In addition, the frame beams are casted by reinforced concrete and fixed on the slope surface, which mainly plays the role of surface protection and transmission of landslide thrust to deep anchor solids. Compared with the traditional slope anchoring method, this new structural reinforcement technology greatly improves the safety and durability of anchorage. The structure of prestressed the grouting steel anchor tube and its reinforcement mechanism is shown in Figure 2.

4. Design of Model Test

4.1. Design of Similitude Relationship. The rational use of similar materials plays a decisive role in the success of model tests [33]. The parameters of similar materials in the landslide physical model mainly include geometric similarity ratio, density, cohesion, internal friction angle, bulk density, and permeability coefficient [27, 28]. Due to the limitations of existing test conditions, this study mainly considers the geometrical similarity parameters, cohesion, internal friction angle, density, and bulk density of materials. Since the longitudinal height of the selected section is 65 m, combined with the size of the existing model box ($h = 1.5$ m), the similarity coefficient of geometric conditions was

$$C_L = \frac{L_P}{L_M} = 50, \tag{1}$$

which C_L is the geometric similarity coefficient, L_M is the model size, and L_P denotes the prototype size of the side slope.

According to the similarity theory, and referring to previous studies of scholars [27, 28], the density similarity ratio (C_ρ) and bulk density (C_γ) are both 1, and the geometric similarity ratio (C_L) is 50 in this landslide physical model. Based on the dimensional analysis method, the similarity ratios of the angle of internal friction (φ) and cohesion (c) are determined as $C_\varphi = 1$, $C_c = 50$.

Based on the above derivation results of similar materials, combined with [34] the orthogonal design of the rock similar material ratio research, determination of the similar

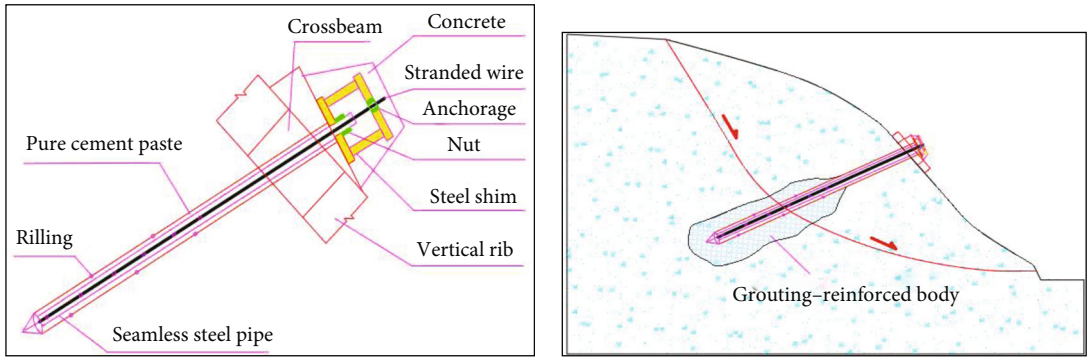

(a) (b)

Figure 2: Structure and reinforcement mechanism of prestressed steel anchor tube frame beam. (a) Prestressed grouted steel anchor tube frame beam structure [32]. (b) Reinforcement mechanism of prestressed grouted steel anchor tube frame beam.

Table 1: Physical and mechanical parameters of prototype and model landslides.

Types	Mechanical parameters	γ (kN/m^3)	ρ (g/cm^3)	c (kPa)	φ (°)
Slide body	Prototype	23.5 ~ 27.4	2.55	/	40
	Model	23.5	2.55	29.91	40.42
Slip band	Prototype	/	/	20	10.5
	Model	/	/	20.43	10.38
Slide bed	Prototype	22.0 ~ 29.0	2.2 ~ 3.0	/	45
	Model	23	2.58	6.29	45.02

Table 2: Mechanical properties and geometric similarity parameters of protection structures.

Protection structure	Profile	Materials	Mechanical parameters	Geometric parameters
Steel anchor tube	Prototype	Steel tube	f_y = 325 MPa	L = 23 m
	Model	PVC tube	f_y = 60 MPa	L = 46 cm
Anchor cable of steel anchor tube	Prototype	Unbonded steel strands	f_y = 1860 MPa	Φ = 15.24 mm, L = 23 m
	Model	Threaded rod	f_y = 335 MPa	Φ = 6 mm, L = 46 cm
Antislide pile	Prototype	C30 concrete	$E_c = 3 \times 10^4$ MPa	$L \times B \times H = 2 \times 2.5 \times 29$ m
	Model	Galvanized square steel tube	$E = 2.06 \times 10^5$ MPa	$L \times B \times H = 4 \times 5 \times 8$ cm
Frame beam	Prototype	C25 concrete	$E_c = 2.8 \times 10^4$ MPa	$B \times H = 0.4 \times 0.3$ m
	Model	Pine	$E = 1.1 \times 10^4$	$B \times H = 0.8 \times 0.6$ cm
Anchor cable of the antislide pile	Prototype	Unbonded steel strands	f_y = 1860 MPa	L = 30 m
	Model	Threaded rod	f_y = 335 MPa	Φ = 6 mm, L = 60 cm

material proportion of model sliding bed, sliding zone, and sliding body by orthogonal matching ratio and indoor direct shear test, coarse sand: soil : cement : water = 30 : 20 : 30 : 10 is used to simulate sliding bed; quartz sand: soil : talc powder : water = 21 : 32 : 50 : 20 is used to simulate the sliding belt; quartz sand: soil : gypsum : water = 40 : 80 : 30 : 10 is used to simulate sliding body. The specific parameters are shown in Table 1.

It is necessary to find appropriate structurally similar materials before carrying out model tests. Because of the difference in mechanical properties of different simulated objects, the selection of similar materials should comply with different similarity requirements, according to the main mechanical properties of the supporting structure in the reinforcement process. In this model test, the tensile strength of the steel anchor tube and anchor cable is used

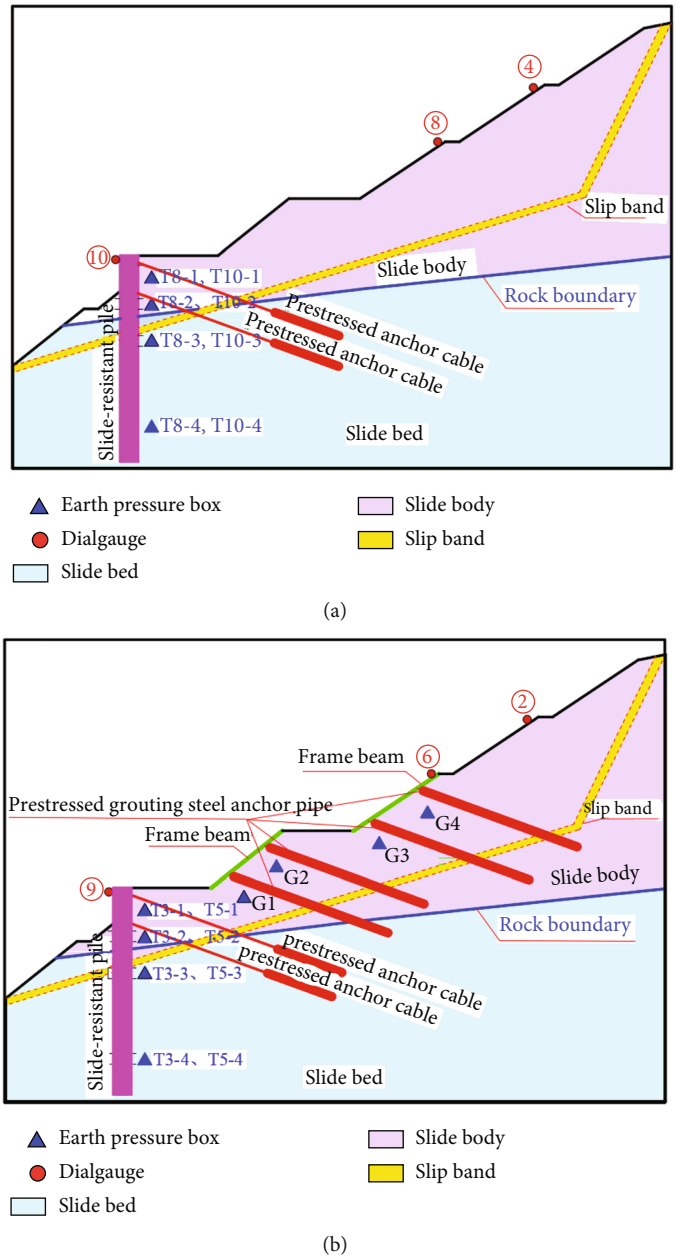

Figure 3: Layout of measuring instruments. (a) The side of setting the prestressed grouting steel anchor tube frame beam. (b) The side of without the prestressed grouting steel anchor tube frame beam.

as the control parameter of similar material, and the bending strength of the frame beam and the antislide pile is used as the control parameter of similar material.

Because it is difficult to realize the absolute similarity selection of the mechanical parameters, the selection of similar materials for protection structures in this model test is mainly based on the geometric similarity constant of the material. To consider the mechanical parameters of materials, the protection structure similar to material selection was determined. The mechanical properties and geometrically similar parameters of the protection structure are shown in Table 2.

4.2. Design of Rainfall. According to China's National Emergency Broadcasting and the Forecast information of Yunnan Meteorological Observatory, the daily rainfall can be as high as 80~120 mm in some areas. Refer to He et al. [35] for the conversion method of rainfall similarity relationship, model rainfall intensity q_m: prototype rainfall intensity $q_p = 1: \sqrt{C_L}$, get the model rainfall intensity $q_m = 11.31 \sim 16.97$ mm. According to the model rainfall time similarity relation $t_m : t_p = 1: \sqrt{C_L}$, the model rainfall time $t_m = 3.39$ h was obtained. Considering the weak response of slope to rainfall under strong support and combining with the rainfall intensity design value of [36] in the model test

Figure 4: Model filling process.

research (the rainfall intensity design value is 30 mm/h). This test enlarges rainfall intensity and shortens rainfall time appropriately. Therefore, the average rainfall intensity of the test design was 32 mm/h, the accumulated rainfall time was about 3 h, and the accumulated rainfall was 96 mm. We adopt the method of controlling the total rainfall constant and intermittent rainfall to better restore the real situation of rainfall.

4.3. The Layout of Measuring Instruments. The sliding displacement of the slope was recorded by using dial gauge displacement meters. On the side of the composite structure with prestressed grouting steel anchor tube frame beam, along the axis of the T4 antislide pile, deploy dial gauge displacement meters on the top of the T4 antislide pile, the fourth-level slope, and the fifth-level slope, respectively. On the side of without the prestressed grouting steel anchor frame beam, along the axis of the T7 antislide pile, deploy dial gauge displacement meters on the top of the T7 antislide pile, the fourth-level slope and the fifth-level slope, respectively. Four earth pressure boxes were installed at different depths behind T3, T5, T8, and T10 antislide piles to monitor the change of earth pressure behind the piles. And the earth pressure boxes were arranged under the steel anchor tubes of the third-level and fourth-level slopes to monitor the change of earth pressure under the steel anchor tubes. The layout of the sensor is shown in Figure 3.

4.4. Model Building. To better restore the prototype of the slope, the process of filling the model from bottom to top is followed, and the slope is divided into two sides along the central line and filled synchronously. One side is equipped with the prestressed grouting steel anchor tube frame beam. And the other side is not equipped with prestressed grouting steel anchor tube frame beam. In addition, the sample material was filled in layers and filled into the model box in the form of 10 cm thick soil layers, and each layer was compacted in the same way to ensure that the model was uniform. The specific process of model making is as follows: preparation of similar materials ⟶ fill the slide bed ⟶ install the prestressed anchor cable antislide pile and the earth pressure after the pile ⟶ fill the slide belt ⟶ fill the slide body ⟶ install the steel anchor tube and the earth pressure at the third-level and fourth-level slope ⟶ fill the slide body of the fifth-level and sixth-level slope ⟶ install the frame beam ⟶ grouting for steel anchor pipe ⟶ maintenance of grouting ⟶ prestressing for steel anchor pipe and anchor cable ⟶ install the dial indicator⟶ install the rainfall device ⟶ connect the sensor to the data collector ⟶ debugging test equipment. The process of model filling was shown in Figure 4. And the complete model was shown in Figure 5.

5. Results and Discussion

5.1. Analysis of the Experimental Phenomenon. The appearance of the progressive destruction process phenomenon of the slope under the action of rainfall was shown in Figure 6. As can be seen from Figure 6, the deformation and destruction of the slope gradually intensified with the continuous progress of rainfall, at 14 : 41, the accumulative rainfall was 24.5 mm, and microcracks first appeared on the slope of the fifth level. The rain lasted for five minutes until 14:26, and the accumulative rainfall reached 29.5 mm. A small collapse and grooves occurred on the side of the prestressed grouting steel anchor tube frame beam on the fourth-level slope. At 15 : 15, the accumulative rainfall has increased to 49.5 mm and then microtension cracks appeared on the platform of the six-level slope. At 15 : 49,

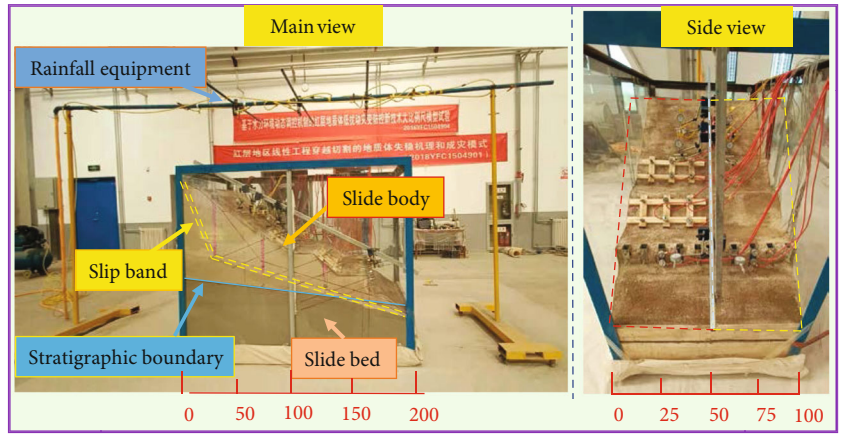

Figure 5: Complete physical model diagram before the test (the unit of dimension in the figure is cm).

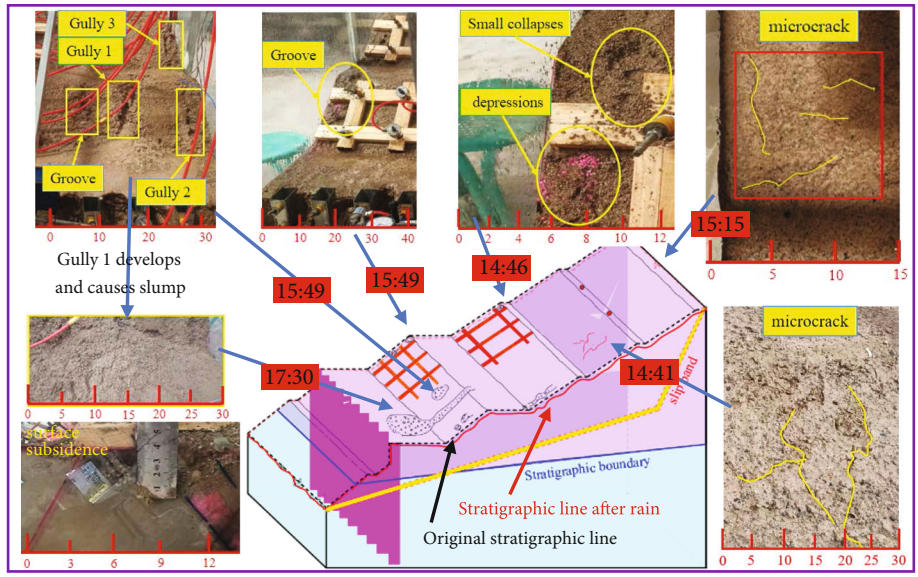

Figure 6: Coevolution process of slope and protective structure under the action of rainfall (the unit of dimension in figure is cm).

the accumulated rainfall amounted to 74 mm on the left side of the frame beam of the third-level slope, local slump, and grooves developed. At the same time, the side grooves of the prestressed grouting steel anchor tube on the third-level slope were extremely developed, and the dissolution gullies 1 and 2 are gradually formed. On the fourth-level slope, the soil loss on the side without the prestressed grouting steel anchor tube gradually developed to form a gully 3. At 17 : 30, a large amount of soil collapsed on the side of the third-level slope without prestressed grouting steel anchor tubes, transporting and depositing on the slope foot under the action of rainfall. And the phenomenon of ground settlements appeared on the slope surface. Obviously, a significant difference in the damage degree of the slope on the side where the prestressed grouting steel anchor tube frame beam was installed and the side where was not installed. Mainly as follows, on the side of without the prestressed grouting steel anchor tube frame beam: rain washes and erodes slopes ⟶ crack appeared on the slope surface ⟶ the slope has developed dissolution grooves and ground settlements ⟶ grooves develop to form gullies ⟶ partial gullies development caused slumping ⟶ the pile is deformed by the extrusion of the soil; on the side of the prestressed grouting steel anchor tube frame beam: rain washes and erodes slopes ⟶ a few microcracks appear on the slope surface ⟶ the slope has developed dissolution grooves ⟶ local collapse and ground settlements occurred. Obviously, the deformation and failure degrees of the side slope were small, which indicates that the prestressed grouted steel anchor tube frame beam had a good effect on slope reinforcement and protection.

5.2. Analysis of Earth Pressure behind Prestressed Anchor Antislide Pile. To understand the response of prestressed anchor cable antislip piles under prestressed grouted steel anchor tube frame beams to slope compression during rainfall. We draw the curves of the peak earth pressure after T3, T5, T8, and T10 piles with the change of buried depth as

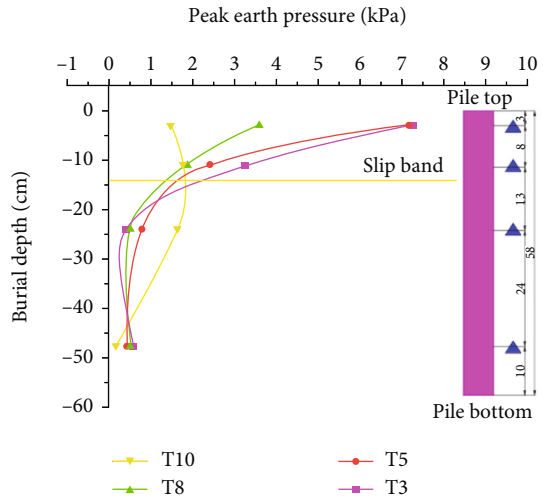

(a) The variation curve of peak earth pressure behind pile with buried depth

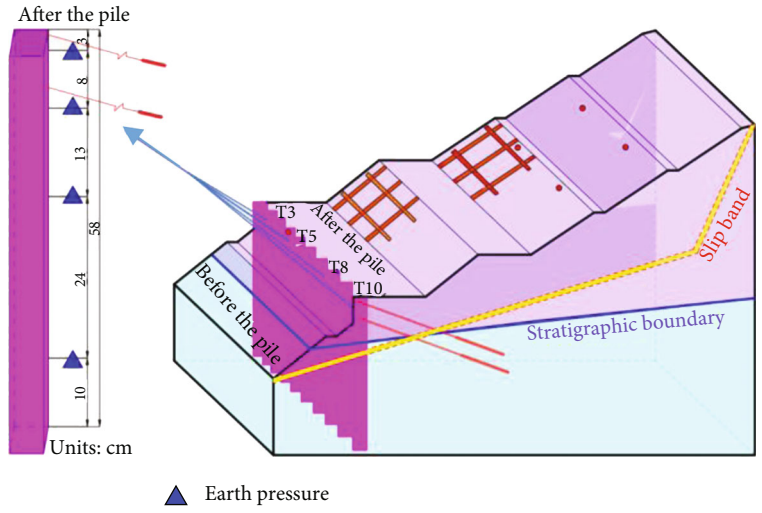

(b) Layout of earth pressure box behind prestressed anchor cable antislide pile

Figure 7: The variation curve of peak earth pressure behind pile with buried depth.

shown in Figure 7. From Figure 7, the earth pressure behind the pile was negatively correlated with the buried depth and generally showed a trend of decreasing with the increase of the buried depth. And the peak earth pressure behind the pile near the surface was the largest, showing that under the action of rainfall, the soil bulk density and the slope weight and the diagonal component increase. And the near-surface section behind the prestressed anchor antislide pile responded most obviously to the sliding force of the slope, which was the main bearing part of the slope sliding force. It is suggested that the stiffness of the near-surface pile should be appropriately increased in practical engineering activities under similar conditions to improve its bearing capacity. In addition, from Figure 7, the peak earth pressure behind the pile near the sliding zone is significantly less than that near the surface, regardless of whether there is prestressed the grouting steel anchor tube frame beam on the slope. It is speculated that the reason for the above phenomena is as follows: in the process of rainfall, the soil bulk density near the surface increases first due to the influence of rainfall infiltration before the overall sliding of the slope occurs. As a result, the earth pressure box near the surface is first squeezed by the soil, so the response of the earth pressure near the surface behind the pile is the most positive.

5.3. Analysis of Earth Pressure under Prestressed Grouting Steel Anchor Tube. The change of the earth pressure curve under the steel anchor tube under the action of rainfall is shown in Figure 8. The earth pressure phases are clearly divided, and the earth pressure variation curve with time under the action of rainfall is mainly divided into four phases in Figure 8. Stage 1: the earth pressure is positively correlated with the accumulated rainfall, which is manifested as a continuous increase with the increase of the accumulated rainfall. The reason for this phenomenon is rainfall infiltration, causing the bulk density of the soil to increase, thereby increasing the oblique force component of the slope, the earth pressure box is increased by the extrusion effect, and the earth pressure curve shows a gradually increasing trend. Stage 2: the accumulated rainfall remains unchanged,

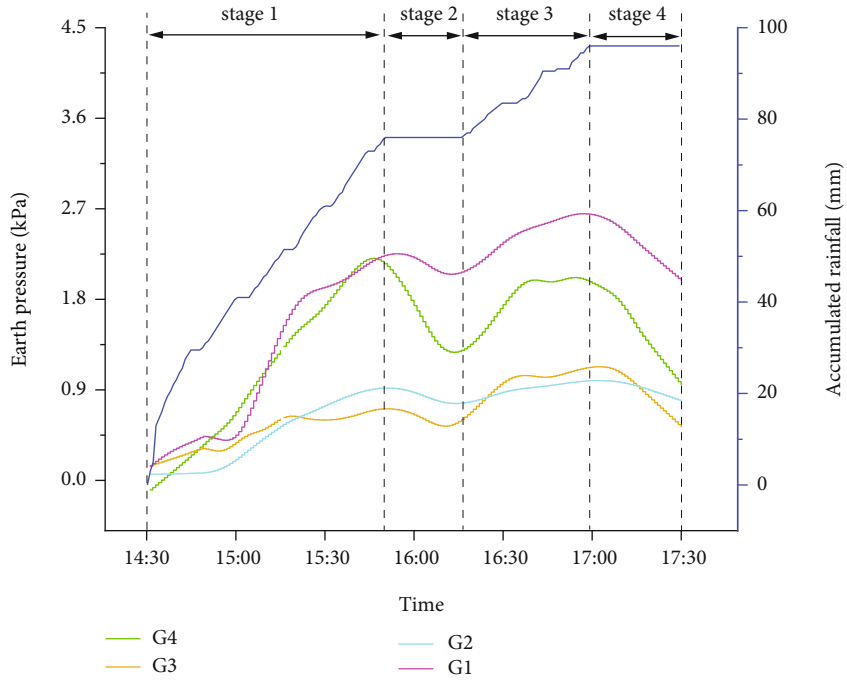

(a) Earth pressure curve under steel tube

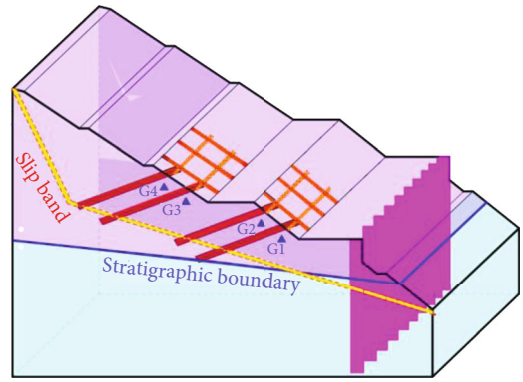

(b) Earth pressure under prestressed grouting steel anchor tube

Figure 8: Earth pressure curve under prestressed grouting steel anchor tube.

meaning the rainfall is 0, and the earth pressure shows a trend of gradual decrease. Combined with the actual test phenomena observed, it can be seen that some rainfall did not penetrate into the soil during the test, but scoured the slope surface to form a gully and flowed away along the gully during the test. In addition, after the rainfall stopped, the rainwater on the slope surface and the local area within the slope continued to accumulate and run off in the gully. It is speculated that the reason for this phenomenon of stage 2 is that the rain stopped, which caused the soil bulk density to decrease, which in turn led to the decrease of the slope component force and the soil rebound. The squeezing effect decreases on the earth pressure box, so the earth pressure curve shows a decreasing trend. Stage 3: the rainfall continues and the earth pressure increases again, repeating the changing trend of stage 1. Stage 4: the accumulated rainfall remained unchanged, and the earth pressure showed a decreasing trend, which repeated the change characteristics of stage 2. Based on the above analysis and combined with the earth pressure curve can be seen, there is a positive correlation between earth pressure and accumulated rainfall. It shows that the magnitude of earth pressure is mainly controlled by rainfall, which is the initiating factor of earth pressure changes.

5.4. Analysis of Displacement Data. The synergistic deformation evolution process of slope and protective structure under rainfall was shown in Figure 9. The displacement monitoring point was shown in Figure 9(a). From Figure 9(b), the slope deformation process under rainfall can be divided into three stages, including the creeping stage: the slope deformation and displacement under the action of rainfall increased slowly. Extrusion stage: the accumulated rainfall continued to increase, the deformation displacement of the slope slowly increases, and the antislide body in the front of the landslide has been compressed. Fretting to

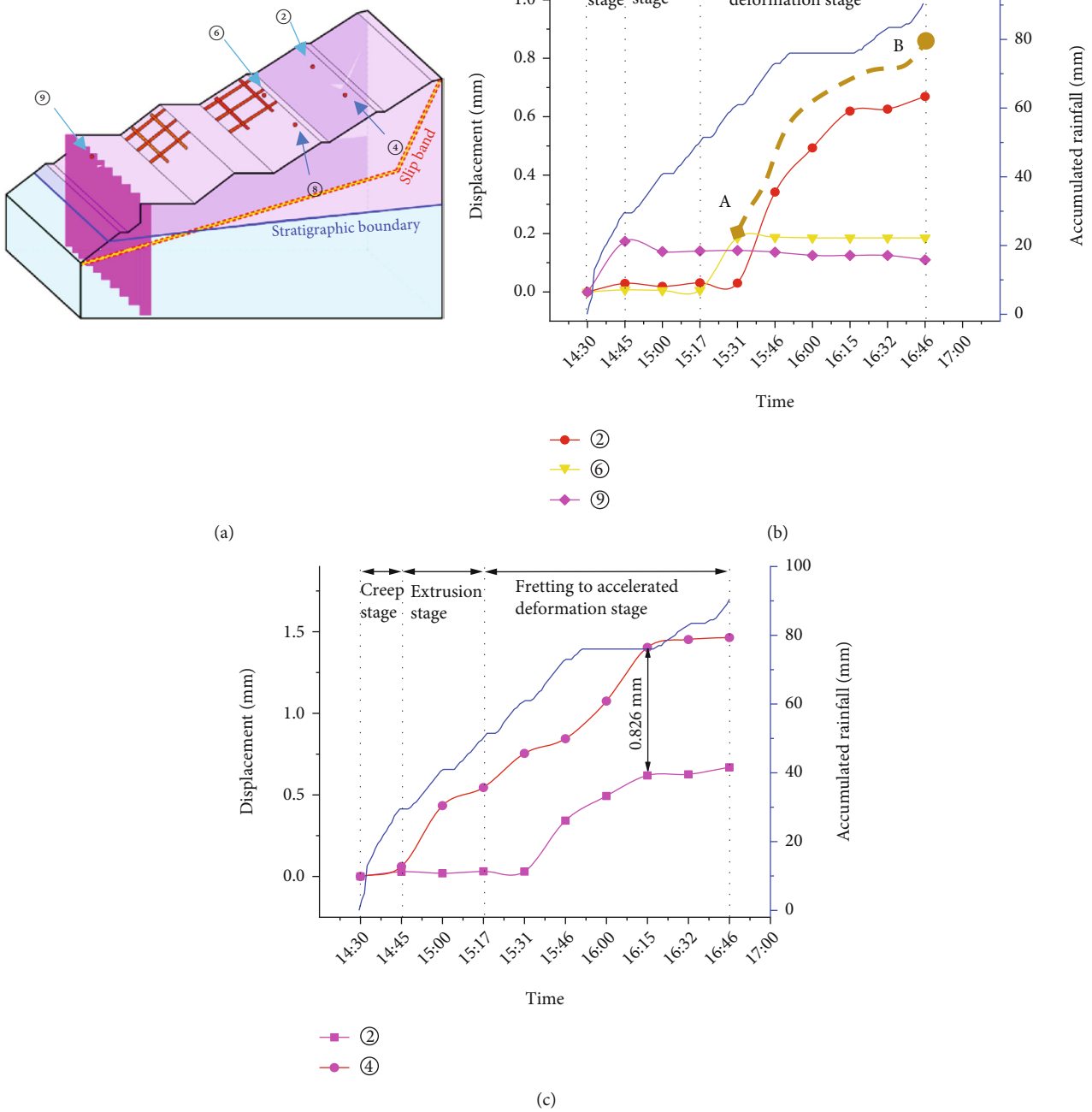

Figure 9: Continued.

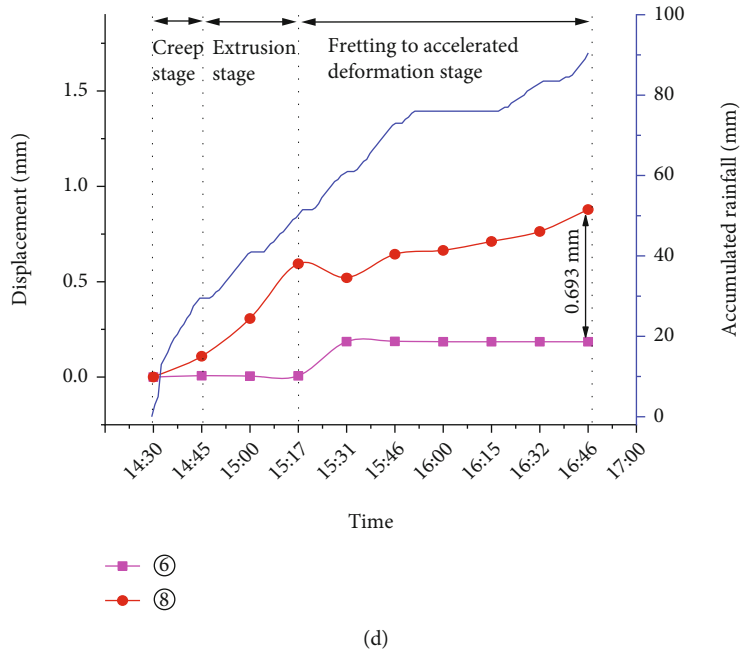

(d)

Figure 9: Deformation displacement curve (a). Layout of measuring points (b). The deformation displacement curve of setting the prestressed grouting steel anchor tube side (c). Comparison of deformation displacement curves of the five-level slope (d). Comparison of deformation displacement curves of the four-level slope.

accelerated deformation stage: when the accumulated rainfall reaches a certain value, the deformation degree intensifies and then enters the fretting to accelerated deformation stage. One of the special phenomena was that after a short period time from fretting to accelerated deformation, the phenomenon of measuring point 6 from fretting to accelerated deformation disappears. The reason for this phenomenon is that the measuring point is within the reinforcement range of prestressed grouting steel anchor tube frame beam, and the reinforcement of supporting structure plays a role. It is predicted that if there is no prestressed grouting steel anchor tube frame beam, measuring point 6 will show the development trend of the AB section. Showing that prestressed grouting steel anchor tube frame beam has a good inhibitory effect on slope deformation displacement. In addition, at the measuring point ⑨ (the top of the T4 pile), the pile tip was squeezed by soil due to the increase of soil weight from rainfall infiltration. And there was a little displacement change at the beginning; then, the soil in front of the pile was compacted to produce resistance. The reinforcement effect of the pile was exerted and the slope deformation was controlled. It is found that under the action of continuous rainfall compared ② and ④ with ⑥ and ⑧, respectively; there is a significant difference in the deformation and displacement of the side slope of the prestressed grouting steel anchor tube frame beam side and the nonprestressed grouting steel anchor tube frame beam side (Figures 8(c) and 8(d)). The maximum displacement difference of ⑥ and ⑧ is 0.693 mm, and the maximum displacement difference of ② and ④ is 0.826 mm. It is further proved that the superior reinforcement effect of prestressed grouting steel anchor tube frame beam composite structure is remarkable for controlling the deformation displacement of the slope.

5.5. Correlation Analysis of the Coevolution of Slope and Protection Structure Based on Multivariate Data Fusion. To further study the relationship between the slope and the prevention structure, we draw the typical deformation displacement curve of the slope, the earth pressure curve behind the pile, the earth pressure curve under the prestressed grouting steel anchor tube, and the cumulative rainfall curve (Figure 10). From Figure 10, the antisliding force provided by the prevention structure is different in the three-stage process of slope deformation under the action of rainfall. When the slope is in the creeping stage, the earth pressure on the side of the pile and under the steel anchor tube is relatively small, showing the antisliding force provided by the prevention structure is relatively small. The slope deformation entered the extrusion stage, the earth pressure behind the pile, and the earth pressure under the prestressed grouting steel anchor tube increased slowly, and there were obvious signs of increase relative to the creeping stage, indicating that under the action of rainfall the antisliding force increasing provided by the prevention structure is obviously when the slope deformation enters the compression stage. As the slope deformation entered the stage of fretting to accelerated deformation, the earth pressure behind the pile increases rapidly, from 0.29 kPa to 1.32 kPa, which was nearly 4.5 times that of the compression stage. Similarly, the increase of earth pressure under the steel anchor tube was relatively obvious, from 1.59 kPa to 2.57 kPa, meaning that under the action of rainfall after the

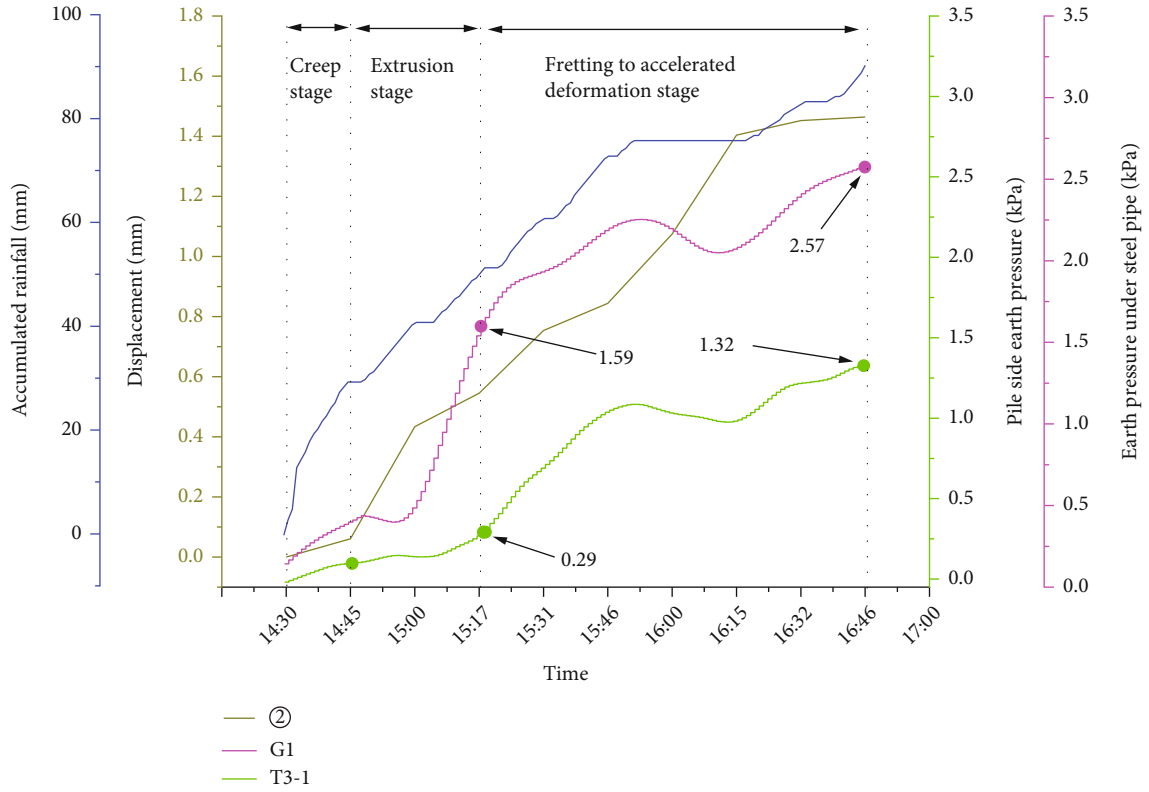

Figure 10: The correlation curve of slope and protective structure under rainfall.

slope deformation enters the stage of fretting to accelerated deformation, the prevention structure needed to provide greater antisliding force.

6. Conclusions and Recommendations

To study the coevolution mechanism between the slope and the prevention structure under the action of rainfall and verify the reinforcement effect of the prestressed grouting steel anchor tube frame beam. First, analyzing the engineering geological characteristics of the prototype diseased slope and concluding that the main inducing factor for the further development of the diseased slope to form a landslide was rainfall. Based on this, building the coevolution model of the slope and the prevention structure under the action of rainfall through indoor model tests, simulating the coevolution process of slope and control structure under the action of rainfall. The conclusion is as follows:

(1) The prestressed grouting steel anchor tube frame beam had a good reinforcement and protective effect on the slope. In this case, the slope deformation displacement and damage degree are significantly different with or without prestressed grouting steel anchor tube frame beam. The deformation and failure degrees of the side slope of the frame beam structure with prestressed grouting steel anchor tube were weak, while the deformation and failure of the side slope without the structure were severe

(2) The evolution process of the deformation displacement of the slope under the action of rainfall is divided into three stages: creeping stage ⟶ extrusion stage ⟶ fretting to accelerated deformation stage. When the slope deformation is in the creeping stage, the earth pressure behind the pile is relatively small, and the antisliding force provided by the prevention structure is relatively small. When the slope deformation enters the extrusion stage, the earth pressure behind the pile is increase slowly, and the antisliding force provided by the prevention structure also increases slowly. When the slope deformation enters the stage of fretting to accelerated deformation, the earth pressure behind the pile increases rapidly, which is about 4.5 times that of the extrusion stage, and it indicates that the prevention structure needs to provide greater antisliding force

(3) The relationship between earth pressure and rainfall under prestressed grouting steel anchor tube in slope was revealed; rainfall was the initiating factor for changes in earth pressure, and the variation of earth pressure under prestressed steel anchor tube frame beam was mainly controlled by rainfall and was positively correlated with accumulated rainfall. In addition, under the action of rainfall, the earth pressure behind the prestressed anchor cable antisliding pile was negatively correlated with the buried depth, which decreased with the increase of the buried

depth, and the peak value of the earth pressure behind the pile near the surface was the largest

(4) Revealing the correlation between the deformation displacement of the slope and the protective structure under the action of rainfall. The antisliding force provided by the prevention structure was positively correlated with the slope deformation. The antisliding force provided by the prevention structure was increasing in varying degrees with the increasing deformation of the slope

Data Availability

The data used to support the findings of this study are available from the corresponding authors upon request.

Conflicts of Interest

The authors declare that they have no competing interests.

Acknowledgments

This research was supported by the National Key R&D Program of China (2018YFC1504904), the National Natural Science Foundation of China (42002280), the Science and Technology Program of Guizhou Province ([2019]1056), science and technology program of Gansu Province (no. 21JR7RA739), and Natural Science Foundation of Gansu Province (No.145RJZA068); and the authors sincerely appreciate the Broadvision Engineering Consultants for the geological survey information, Dr. Yuan Kun to provide modification advice, and Mr. Pang Jun to provide test help on this work.

References

[1] J. S. Gidon and S. Sahoo, "Rainfall-induced slope failures and use of bamboo as a remedial measure: a review," *Indian Geotechnical Journal.*, vol. 50, no. 5, pp. 766–783, 2020.

[2] C. Sidleroy and T. A. Bogaard, "Dynamic earth system and ecological controls of rainfall-initiated landslides," *Earth Science Reviews*, vol. 159, pp. 275–291, 2016.

[3] S. A. Benz and P. Blum, "Global detection of rainfall-triggered landslide clusters," *Natural Hazards and Earth System Sciences*, vol. 19, no. 7, pp. 1433–1444, 2019.

[4] Q. Wang, H. Ye, N. Li et al., "A study of support characteristics of collaborative reinforce system of U-steel support and anchored cable for roadway under high dynamic stress," *Geofluids*, vol. 2021, Article ID 9881280, 12 pages, 2021.

[5] S. Wang, G. Li, J. Tan et al., "Multi-index monitoring and comprehensive early warning analysis of landslide response to rainfall: an example of Luoao landslide in southern Jiangxi Province," *Earth Science Frontiers*, vol. 28, pp. 1–15, 2021.

[6] Y. Wang, M. Han, X. Lin, D. Li, H. Yu, and L. Zhu, "Influence of rainfall conditions on stability of slope reinforced by polymer anti-slide pile," *Earth Science.*, vol. 9, 2021.

[7] G. Shi, G. Gu, H. Zhou et al., "Stability monitoring and analysis of high and steep slope of a hydropower station," *Geofluids*, vol. 2020, Article ID 8840269, 16 pages, 2020.

[8] E. Ausilio, E. Conte, and G. Dente, "Stability analysis of slopes reinforced with piles," *Computers and Geotechnics*, vol. 28, no. 8, pp. 591–611, 2001.

[9] F. Cai and K. Ugai, "Numerical analysis of the stability of a slope reinforced with piles," *Soils and Foundations*, vol. 40, no. 1, pp. 73–84, 2000.

[10] F. Cai and K. Ugai, "Reinforcing mechanism of anchors in slopes: a numerical comparison of results of LEM and FEM," *International Journal for Numerical and Analytical Methods in Geomechanics*, vol. 27, no. 7, pp. 549–564, 2003.

[11] B. D. Nath, M. K. A. Molla, and G. Sarkar, "Study on strength behavior of organic soil stabilized with fly ash," vol. 2017, Article ID 5786541, pp. 1–6, 2017.

[12] C. Y. Chen and G. R. Martin, "Soil-structure interaction for landslide stabilizing piles," *Computers and Geotechnics*, vol. 29, no. 5, pp. 363–386, 2002.

[13] T. Li, X. Tian, W. Han, Y. Ren, Y. He, and Y. Wei, "Centrifugal model tests on sliding failure of a pile-stabilized high fill slope," *Rock and Soil Mechanics*, vol. 34, no. 11, pp. 3061–3070, 2013.

[14] J. Ma, H. Tang, X. Hu et al., "Model test study of surface displacement field of slope stabilized with anti-sliding piles," *Chinese Journal of Rock Mechanics and Engineering*, vol. 33, no. 4, pp. 679–690, 2014.

[15] X. Xu, Y. Xing, Z. Guo, and Y. Huang, "Stability analysis of rainfall-triggered toe-cut slopes and effectiveness evaluation of pile-anchor structures," *Journal of Earth Science*, vol. 32, no. 5, pp. 1104–1112, 2021.

[16] G. Zhang and L. Wang, "Simplified evaluation on the stability level of pile-reinforced slopes," *Soils and Foundations*, vol. 57, no. 4, pp. 575–586, 2017.

[17] H. Chen, G. Zhang, Z. Chang, L. Wen, and W. Gao, "Failure analysis of a highway cut slope with anti-slide piles," *Geofluids*, vol. 2021, Article ID 6622214, 15 pages, 2021.

[18] F. A. B. Danziger, B. R. Danziger, and M. P. Pacheco, "The simultaneous use of piles and prestressed anchors in foundation design," *Engineering Geology*, vol. 87, no. 3-4, pp. 163–177, 2006.

[19] J. Li, S. Chen, F. Yu, and L. Jiang, "Reinforcement mechanism and optimisation of reinforcement approach of a high and steep slope using prestressed anchor cables," *Applied Sciences*, vol. 10, no. 1, p. 266, 2020.

[20] S. Ye, G. Fang, and Y. Zhu, "Model establishment and response analysis of slope reinforced by frame with prestressed anchors under seismic considering the prestress," *Soil Dynamics and Earthquake Engineering*, vol. 122, pp. 228–234, 2019.

[21] Z. Wu, Z. Wang, J. Bi, X. Fu, and Y. Yao, "Shaking table test on the seismic responses of a slope reinforced by prestressed anchor cables and double-row antisliding piles," *Shock*, vol. 2021, article 9952380, pp. 1–13, 2021.

[22] G. Fan, J. Zhang, S. Qi, and J. Wu, "Dynamic response of a slope reinforced by double-row anti-sliding piles and prestressed anchor cables," *Journal of Mountain Science*, vol. 16, no. 1, pp. 226–241, 2019.

[23] S. Fan, Z. Song, Y. Zhang, and N. Liu, "Case study of the effect of rainfall infiltration on a tunnel underlying the roadbed slope with weak inter-layer," *KSCE Journal of Civil Engineering*, vol. 24, no. 5, pp. 1607–1619, 2020.

[24] M. Branco, L. Guerreiro, A. Campos Costa, and P. Candeias, "Shaking table tests of a structure equipped with superelastic dampers," *Journal of Earthquake Engineering*, vol. 18, no. 5, pp. 674–695, 2014.

[25] R. J. Bathurst, S. Zarnani, and A. Gaskin, "Shaking table testing of geofoam seismic buffers," *Soil Dynamics and Earthquake Engineering*, vol. 27, no. 4, pp. 324–332, 2007.

[26] C. Li, W. Zhang, T. Huo, R. Yu, X. Zhao, and M. Luo, "Failure analysis of deep composite roof roadway and support optimization of anchor cable parameters," *Geofluids*, vol. 2021, Article ID 5610058, 13 pages, 2021.

[27] K. Wang, Y. Li, G. Li, and X. Yu, "Experimental study on the horizontal bearing capacity of vertical steel floral tube micropiles with twice grouting," *Chinese Journal of Rock Mechanics and Engineering*, vol. 38, no. 8, pp. 1707–1717, 2019.

[28] K. Wang, Z. Ren, X. Mei et al., "Rainfall difference between the deposition fan and source area of Touzhai landslide in Yunnan, China," *Bulletin of Engineering Geology and the Environment*, vol. 78, no. 3, pp. 1937–1954, 2019.

[29] H. Chen, Y. Zhang, X. Zhang, and S. Wei, "Full-scale model experiments on anti-sliding characteristics of high-pressure grouting steel-tube micropiles," *Rock and Soil Mechanics*, vol. 41, no. 2, pp. 428–436, 2020.

[30] Y. Zhang, S. Wei, W. Zhou, D. Li, and B. Zhou, "Model test study on anti-sliding behaviours of multiple segmented grouting steel pile group structure," *Chinese Journal of Rock Mechanics and Engineering*, vol. 38, no. 5, pp. 982–992, 2019.

[31] W. Zhou, S. Wei, and Y. Zhang, "Model test study on anti-sliding performance of multiple segment grouting steel-tube," *Rock and Soil Mechanics*, vol. 40, no. 11, pp. 4412–4420, 2019.

[32] K. Yuan, Y. Zhang, M. Lei, and L. Cao, "Field test on reinforcement technology of steel anchor pipe and anchor cable composite structure with multi-stage control grouting in inclined direction," *Science Technology and Engineering*, vol. 20, no. 25, pp. 10504–10510, 2020.

[33] Z. Jiang, H. Wang, and W. Xie, "Deformation mechanism of deposit landslide induced by fluctuations of reservoir water level based on physical model tests," *Environment and Earth Science*, vol. 80, no. 11, pp. 1–13, 2021.

[34] Y. Ning, H. Tang, B. Zhang, P. Shen, G. Zhang, and D. Xia, "Investigation of the rock similar material proportion based on orthogonal design and its application in base friction physical model tests," *Rock and Soil Mechanics*, vol. 41, no. 6, pp. 2009–2020, 2020.

[35] Z. He, X. Deng, H. Tang, X. Duan, and H. Bian, "Experiment on spatial and temporal evolution of transient saturated zone of coarse soil high embankment slope under rainfall condition," *China Journal of Highway and Transport*, vol. 31, no. 2, pp. 261–269, 2018.

[36] J. Gan and Y. X. Zhang, "Analysis of model tests of rainfall-induced soil deposit landslide," *Advances in Civil Engineering*, vol. 2020, 13 pages, 2020.